

Study of the Matrix Shrinkage on a Polymer Matrix Composite under a Drop of Temperature

Le Thi Tuyet Nhung, Trieu Van Sinh, Vu Dinh Quy*

Hanoi University of Science and Technology, Hanoi, Vietnam

*Corresponding author email: quy.vudinh@hust.edu.vn

Abstract

A polymer composite material consists of two different phases with very different mechanical properties. Thus, there is a shrinkage when a decrease in temperature appears. This paper focuses on the matrix shrinkage of a unidirectional polymer matrix composite under a temperature drop. A Rayleigh-Ritz method is used to rapidly determine the matrix displacement (matrix shrinkage) field of virgin samples (initial state, without thermo-oxidation). Additionally, numerical simulations are also carried out. A comparison of maximum matrix shrinkages is carried out among the experiment measurement, the Rayleigh-Ritz method, and the numerical simulation method. The numerical results of the matrix displacement are compared to the experiment and the Rayleigh-Ritz method. There is a good correlation between the results obtained by the two methods. Then, an assessment of the reliability of numerical simulations is given. The numerical simulations are then used to analyze the evolution of stress along the different paths on the sample to predict the damage behavior.

Keywords: Rayleigh-Ritz method, matrix shrinkage, composites, numerical simulations, drop of temperature

1. Introduction

Composite materials are widespread used in aerospace industries due to their high specific mechanical properties. To use composite materials in the aerospace structure, researches have been carried out to ensure durability and reliability. The use of composite material in the parts subjected to severe thermal conditions is foreseen and researches about the durability of composite materials in the such thermo-oxidation environment must be implemented. Many researches on thermos-oxidation of polymer matrix composite material were carried out on both chemical aspects [1] and the impact of thermo-oxidative environments on the mechanical degradation of polymer composites has made the object of several research papers [2-4], mainly focusing on the behavior of neat resins and of polymer-matrix composites at the macroscopic scale [5-9].

A few late investigations have focused on carbon-epoxy composites, tending toward the impact of the reinforcement on the debasement of the composite, both at the microscopic and the naturally macroscopic scale. It is asserted that the presence of carbon may change matrix degradation, however, the results of these impacts are not decisive and emphatically rely upon the composite framework.

During the study of the effects of thermal oxidation on organic matrix composites, Vu *et al.* [2] used the interferometric microscopy (IM) for a deep study of matrix shrinkage on the surface of unidirectional IM7/977-2 carbon/epoxy composites

subjected to an aggressive thermal oxidation environment, under air at atmospheric pressure or under oxygen partial pressure (up to 5 bar) and came up with the evolution of matrix shrinkage against oxidation time and the damage development on such composites.

Gigliotti *et al* [3] used a similar methodology for HTS/TACTIX carbon/epoxy composites and this study indicated that matrix shrinkage between fibres increases with oxidation time in resin-rich zones (zones with low fibre volume fraction), leading eventually to the debonding at fibre-matrix interfaces. Since fibres do not deform during oxidation, they constrain the free development of matrix resin shrinkage.

According to another study, Gigliotti *et al* [4] implemented the measurement of matrix shrinkage on the composite surface by using IM for virgin samples (initial state) subjected to a temperature drop from the curing temperature to room temperature. Then, a compilation of data of maximum matrix shrinkage with fibre-to-fibre distance was presented as in Fig. 1. Maximum matrix shrinkages is at the middle of fibre-to-fibre distance.

A Rayleigh-Ritz method is mentioned in Gigliotti's study to rapidly determine this matrix shrinkage field. However, a clearer study of the dependence of this matrix shrinkage against the parameters such as fibre length, Poisson's ratio,

inelastic strain (caused by a temperature difference) has not been made yet.

Therefore, to clarify the thing above, the present paper focuses on investigating the effect of the above parameters on the matrix shrinkage field. The formula of matrix shrinkage (matrix displacement) is proposed to find the maximum matrix shrinkage with each fibre-to-fibre distance. The collection of these maximum matrix shrinkages creates a Rayleigh-Ritz curve which is compared to the experimental data for finding the fibre length H , Poisson's ratio ν , the inelastic strain $\epsilon^{In} = \alpha\Delta T$. Then, numerical simulations of the matrix shrinkage caused by the temperature decrease on 2D and 3D models are implemented to validate the phenomenon and their results are compared to the experiment results and the Rayleigh-Ritz method.

2. Determination of Matrix Shrinkage by Rayleigh-Ritz Method

In [4], Gigliotti *et al* gave the structure for studying the initial shrinkage field (Fig. 2). They came up with a formula of the displacement field of the matrix shrinkage using Rayleigh-Ritz method for the initial state of virgin samples (not aged):

$$\begin{aligned} u(x, y, z) &= 0 \\ v(x, y, z) &= 0 \\ w(x, y, z) &= \frac{30(\nu + 1)\alpha\Delta T}{6L^2(1 - \nu) + 5H^2(1 - 2\nu)} x(x - L)(H - z) \end{aligned} \quad (1)$$

where:

- The coordinate system is presented in Fig. 3.
- The quadratic form in x ensures that the displacement w is zero close fibres (at $x = 0$ and $x = L$),
- ν is the Poisson's ratio ($0 < \nu < 0.5$)
- α is the thermal expansion coefficient
- ΔT is the temperature difference and is a negative value with a temperature decrease, $\epsilon^{In} = \alpha\Delta T$ is the inelastic strain.

This formula is determined by the following hypotheses:

- Fibres are rigid,
- Fibre-matrix links are ignored.

From (1), the maximum matrix shrinkage is at $x = L/2$, $z = 0$ and is determined by the following formula:

$$w_{\max} = \frac{-30(\nu + 1)\alpha\Delta T}{6L^2(1 - \nu) + 5H^2(1 - 2\nu)} \frac{L^2 H}{4} \quad (2)$$

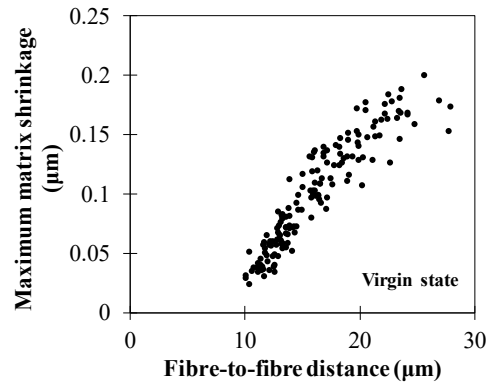


Fig. 1. Maximum matrix shrinkage in the function of the fibre-to-fibre distance on virgin samples.

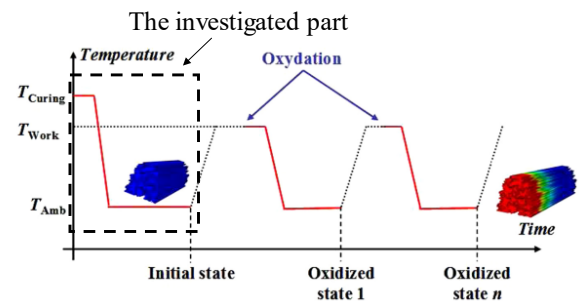


Fig. 2. Structure for studying the initial shrinkage field.

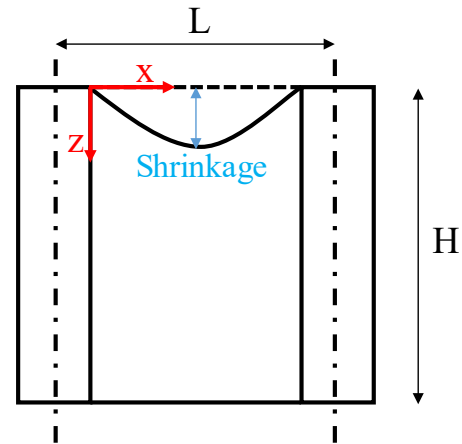


Fig. 3. Schematic representation of matrix shrinkage between fibres.

With each value of H , ν , $\epsilon^{In} = \alpha\Delta T$, L , a value of w_{\max} is determined, the compilation of these w_{\max} creates a Rayleigh-Ritz (RR) curve. The requirement is to find (H , ν , ϵ^{In}) such that this curve is in the distribution area of experiment points and the difference compared to the experiment is minimum. These values of (H , ν , ϵ^{In}) are used in the next section for numerical simulations.

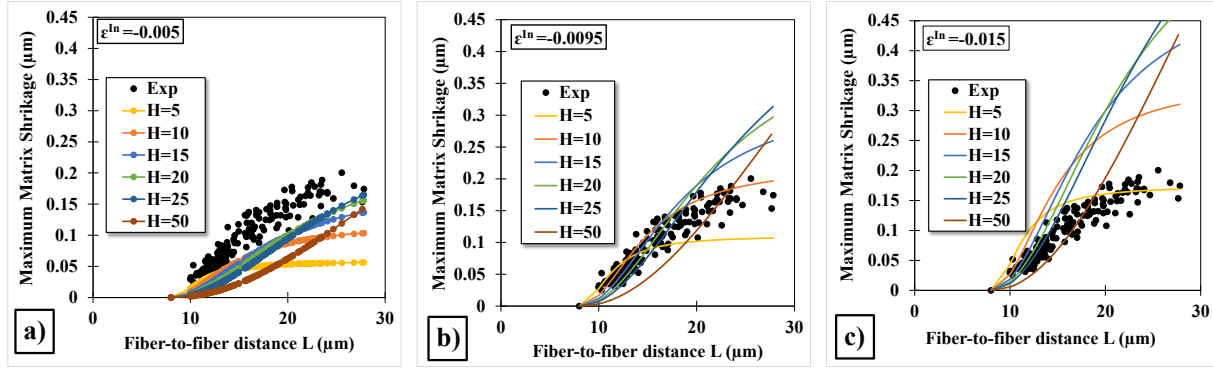


Fig. 4. Evolution of the maximum matrix shrinkage as a function of the fibre-to-fibre distance: a) $\varepsilon^{In} = -0.005$ b) $\varepsilon^{In} = -0.0095$; c) $\varepsilon^{In} = -0.015$.

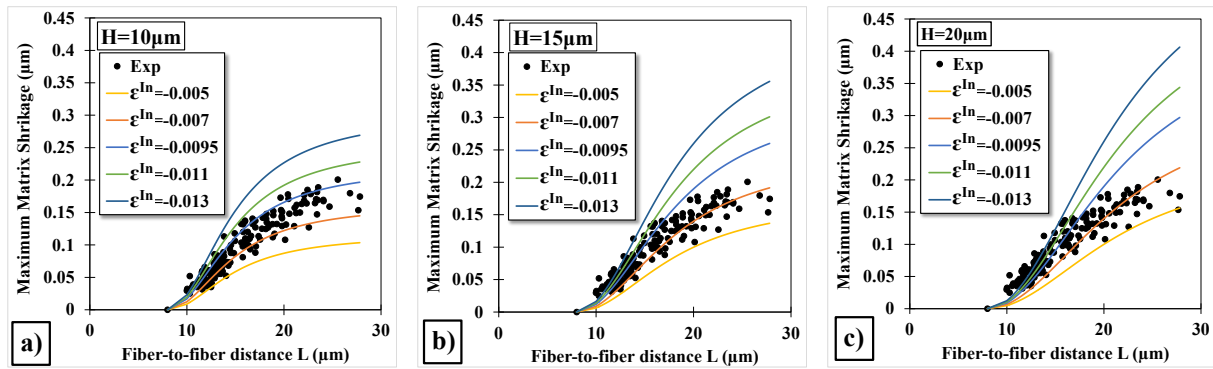


Fig. 5. Evolution of the maximum matrix shrinkage as a function of the fibre-to-fibre distance: a) $H = 10 \mu\text{m}$ b) $H = 15 \mu\text{m}$; c) $H = 20 \mu\text{m}$.

A virgin sample (before aging) is subjected to a temperature drop from $150 \text{ }^\circ\text{C}$ to $20 \text{ }^\circ\text{C}$. This sample has an initial Poisson's ratio $\nu = 0.3$.

Fig. 4 presents three graphs that express the relations between maximum matrix shrinkage curves and the fibre-to-fibre distances. In each graph, the value of inelastic strain ε^{In} is constant, the length of fibre H varies from 5 to 50 μm . Each colorful curve (red, green, yellow...) is a simulation result of RR maximum matrix shrinkages with a value of H fibre-to-fibre distances. Black points represent experiment points. It can be seen that, with $\varepsilon^{In} = -0.005$ and $\varepsilon^{In} = -0.015$, the RR curves are not located in experiment points (located below black points zone with $\varepsilon^{In} = -0.005$, above black points with $\varepsilon^{In} = -0.015$). With $\varepsilon^{In} = -0.0095$, the simulation curves are completely in the zone of experiment points. Especially, with $\varepsilon^{In} < -0.015$, the RR curves tend to diverge (away from the black points). Further, with $H > 50 \mu\text{m}$, the shape of curves begins changing and does not match with the trend of the black points (shrinkages increase slowly when fibre-to-fibre distance increases). So, with $H = 10 \mu\text{m}$, $\varepsilon^{In} = -0.0095$, $\nu = 0.3$, the RR curve

does match approximately the area of the experiment points.

Fig. 5 presents the evolution of maximum matrix shrinkage as a function of the distance between fibres with the increase of the inelastic strain ε^{In} in 3 cases: $H = 10 \mu\text{m}$, $H = 15 \mu\text{m}$, $H = 20 \mu\text{m}$. The curves tend to move up with the increase of the inelastic strain ε^{In} .

Fig. 6 presents the evolution of maximum matrix shrinkage as a function of the distance between fibres in case $H = 10 \mu\text{m}$, $\varepsilon^{In} = -0.0095$ and the change of the value of ν .

From Fig. 7, an evaluation is given that the RR curve matches approximately the experiment points with $H = 10 \mu\text{m}$, $\varepsilon^{In} = -0.0095$, and $\nu = 0.3$. However, this is not the parameters to be found yet because the difference between the RR curve and the experiment is no minimum. The minimum square method is used for minimizing this difference. So, the parameters H , ν , ε^{In} are found respectively 11 μm , 0.33, -0.0073. And the minimum difference is 3.42%.

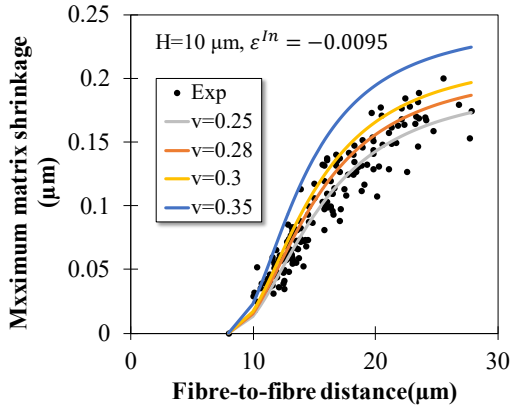


Fig. 6. Evolution of the maximum matrix shrinkage as a function of the fibre-to-fibre distance when $H = 10 \mu\text{m}$, $\epsilon^{In} = -0.0095$, the value of ν changes.

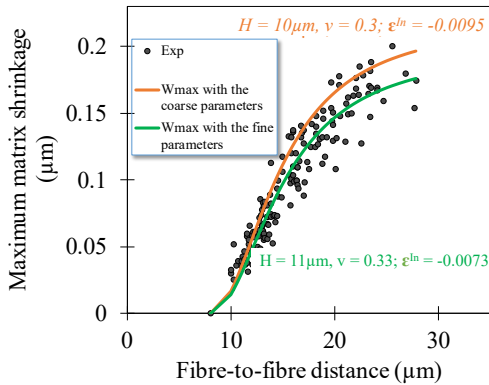


Fig. 7. Maximum matrix shrinkage curve as a function of the distance between fibres with $(H, \nu, \epsilon^{In}) = (10, 0.3, -0.0095)$ and $(11, 0.33, -0.0073)$.

3. Validating the Approach by Simulating Matrix Shrinkage in a Virgin Sample.

Fig. 8a presents the 2D geometry model with a simulated zone that is a $12 \mu\text{m} \times 11 \mu\text{m}$ rectangular. Fig. 8b presents the 3D geometry model with a simulated zone that is the crossed zone. In these 2 cases of the problem, the P point is the considered point. In each case of the distance between fibres of the simulation, a maximum matrix shrinkage at the P point is determined. A collection of these shrinkages creates the maximum matrix shrinkage curve as a function of the distance between fibres.

Table 1 presents the material properties employed in the simulations, where Poisson's ratio $\nu = 0.33$ and the thermal expansion coefficient $\alpha = \epsilon^{In} / \Delta T$.

Table 1. Material properties used in simulations.

Parameter	Value
Young's modulus	3,500 MPa
Poisson's ratio	0.33
Thermal expansion coefficient	$0.0073/130 \approx 5.615385e-5$

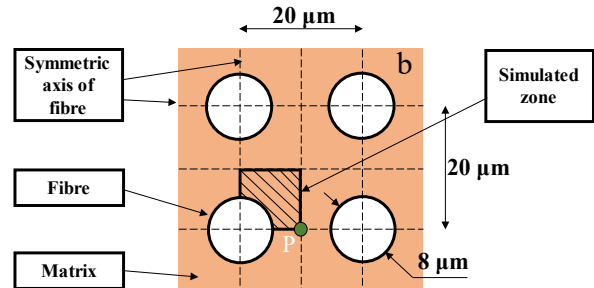
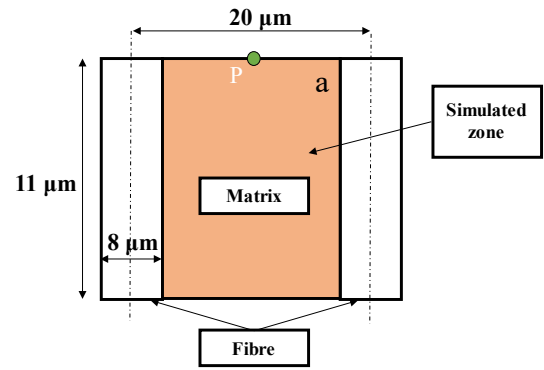


Fig. 8. a) 2D geometry model; b) 3D geometry model

3.1. Geometry Boundary Conditions

To simplify the problem, it is assumed that fibres are rigid, and the fibre-matrix links are ignored. The displacements of the points on the free edge are very small compared to the length of fibres, so the bottom edge is clamped (Fig. 9 and Fig. 10). These boundary conditions are not true to reality; therefore, the results of stress and displacements are not correct. However, with these boundary conditions, the matrix shrinkage phenomenon still appears, and the preliminary evaluation of these shrinkages is given. Besides, the values of the maximum Von-Mises stress at fibre-matrix interface are insignificant in any comparison but it reflects the stress concentration at these positions and is suitable for the experiment images. Especially, the matrix shrinkage mechanism completely is unchanged, and with the overall assessment, these boundary conditions are acceptable.

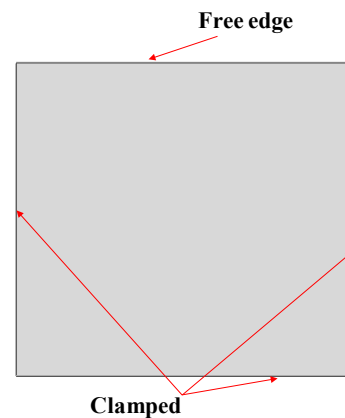


Fig. 9. Boundary conditions in 2D model.

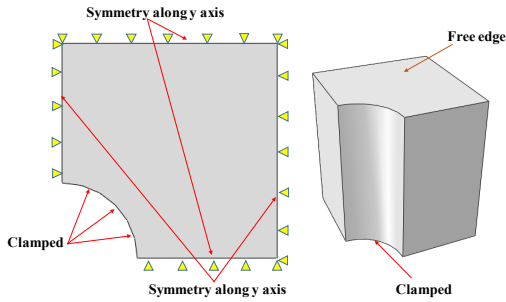


Fig. 10. Boundary conditions in 3D model.

3.2. Temperature Conditions

The composite plate is subjected to a temperature drop from 150 °C to 20 °C, so in step 1, the temperature is 150 °C and in step 2, the one is 20 °C.

3.3. Meshing

In the simulation, considering the mesh element quantity is important because of its effect on numerical results. With a small number of elements, the obtained results are not reliable enough, otherwise, with many elements, the computation time is significant, especially for the 3D simulations or for the problems with fiber-matrix contact.

In 2D simulation, the composite plate is divided into rectangle elements (CPE4R). A mesh convergence investigation is considered to select the number of elements for simulation.

Fig. 11 shows that the Von-Mises stress is almost unchanged since the number of elements is 20000. Then, the value of Von-Mises stress is 159.9 MPa.

With 20000 elements, the value of maximum displacement (maximum shrinkage) of the composite plate at the E point is also unchanged, 1.272e-7 mm (Fig. 12).

Through considering the convergence of meshing, the 2D model used 20,000 CPE4R elements, and the 3D model used 34,960 C3D8R elements for their simulations (Fig. 13).

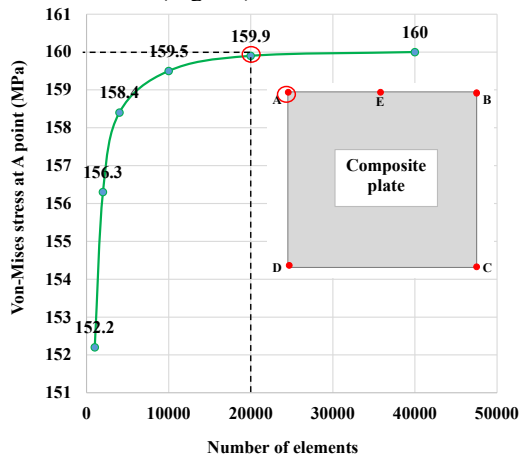


Fig. 11. The graph of the Von-Mises stress at A point and the number of mesh elements.

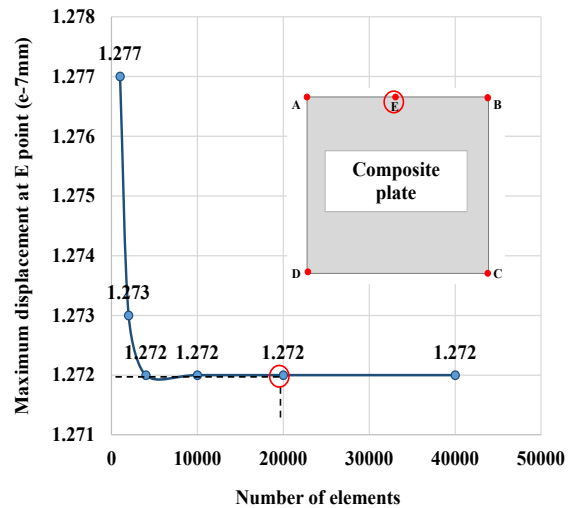


Fig. 12. The graph of maximum displacement at E point and the number of mesh elements.

4. Numerical Simulation Results

4.1. 2D Simulation

The value of the maximum matrix shrinkage is $1.272e-4 \text{ mm} = 0.1272 \mu\text{m}$ at the middle of the free edge (Fig. 14b). This value is very small compared to the length of fibres. Besides, the matrix shrinkage curve is completely similar to the curve's form mentioned in section 2 when the Rayleigh-Ritz method is applied to determine the matrix displacement.

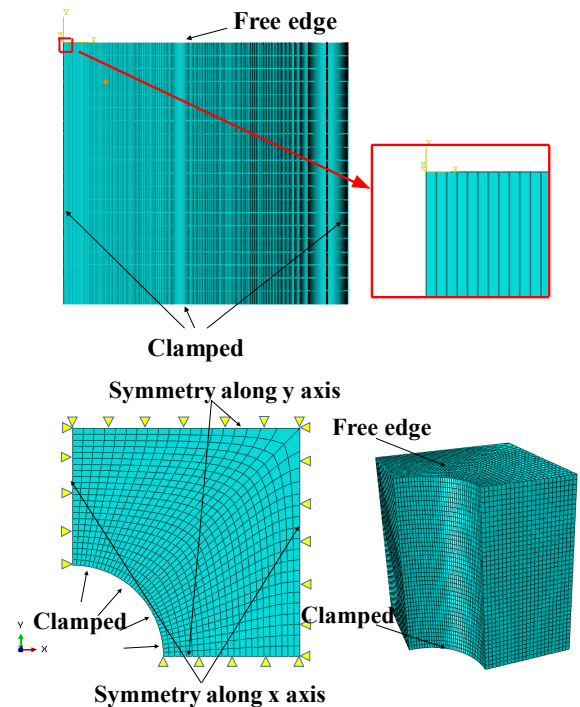


Fig. 13. The graph of the mesh 2D and 3D

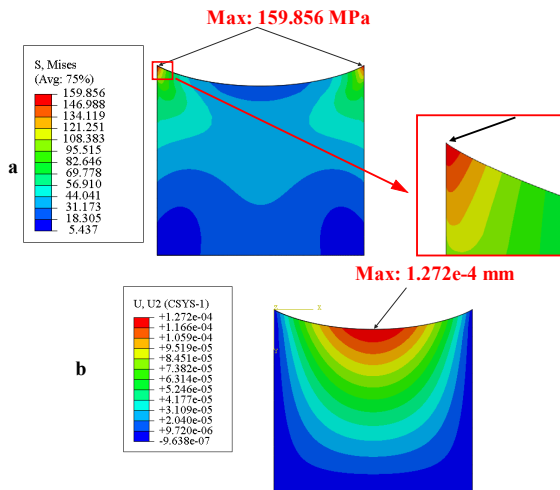


Fig. 14. The distribution of the Von-Mises stress and the matrix displacement on the composite plate

The maximum Von-Mises stress at 2 points which is the intersection of the free edge, and the fibre-matrix interface has a value of 159.9 MPa (Fig. 14a). This is completely apparent because of the boundary conditions. This value suggests that the first damage will occur at these points.

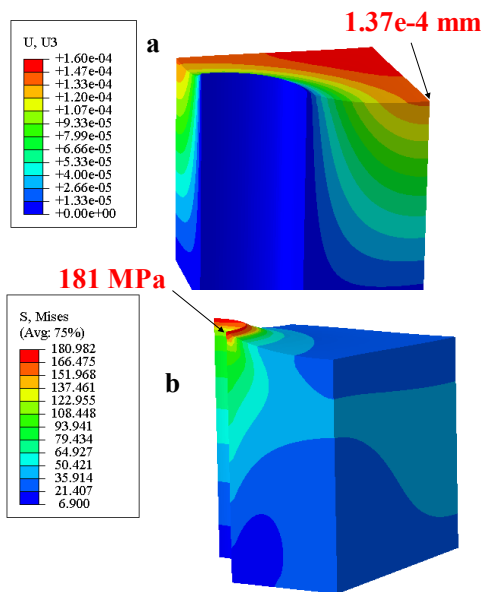


Fig. 15. The distribution of the stress and the matrix displacement on the 3D structure.

4.2. 3D Simulation

Fig. 15a presents the distribution of the matrix displacement along z-axis (U_3) on the whole structure. At the fibre-matrix interface and its vicinity, the values of the displacement are zero. The displacement increases gradually toward the middle of the free edge and reaches the maximum value at this point. This maximum value at the P point is $0.137 \mu\text{m}$. The maximum Von-Mises stress is about 180.9 MPa (Fig. 15b).

Fig. 16a shows that the value of the Von-Mises decreases gradually along the P_2P_1 path. Especially, there is a sudden drop of the stress from P_2 to a point which is $0.002 \mu\text{m}$ away from P_2 . This is easy to explain because P_2 point became a singularity point. A change of the Von-Mises stress along P_2P_3 path is expressed in Fig. 16b.

5. Comparison of Results among Methods

Fig. 17 shows a comparison of the maximum matrix shrinkage in three ways: the experiment, the Rayleigh-Ritz method, and the numerical simulation. The results of the maximum matrix shrinkage in simulations are still in the experiment points, however, there is a significant difference compared to the experiment. Besides, the difference in the results between the Rayleigh-Ritz method and the Abaqus simulation increases with the increase of the fibre-to-fibre distance, and its maximum value is 10%. Remarkably, the maximum difference of the maximum matrix shrinkage in 2D and 3D simulations is 4% - an acceptable difference - at the fibre-to-fibre distance of $22 \mu\text{m}$. This suggests that 2D simulations can be employed instead of 3D simulations so that the obtained results are not much different.

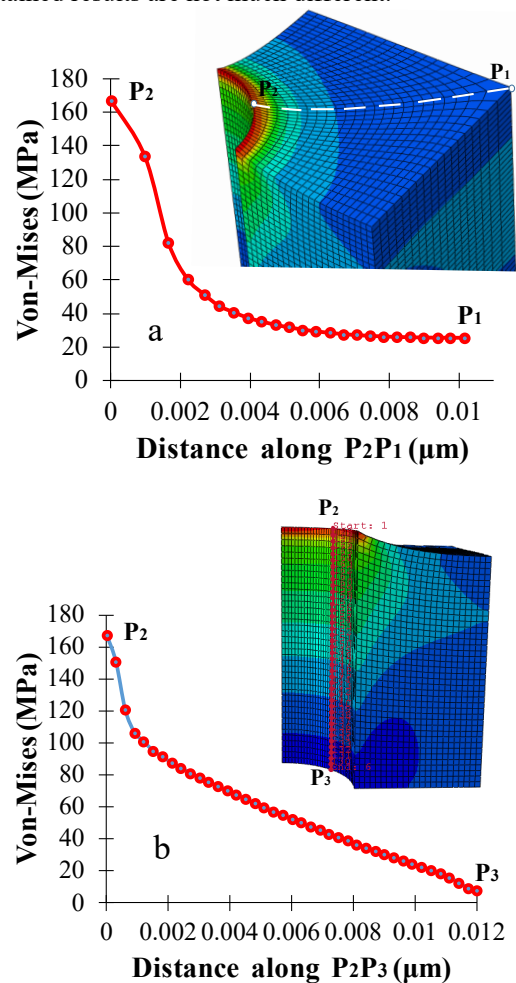


Fig. 16. The Von-Mises stress as a function of the distance along: a) P_2P_1 path; b) P_2P_3 path

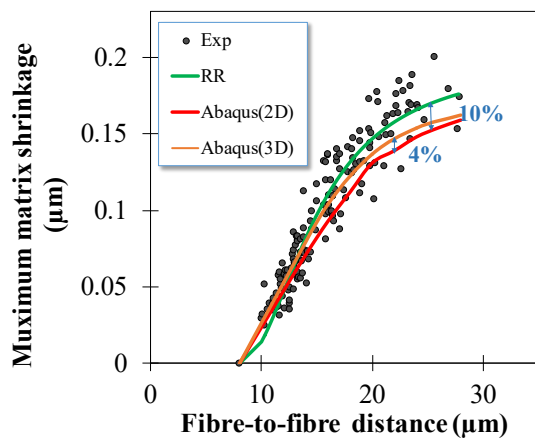


Fig. 17. The comparison of the maximum matrix shrinkage as a function of the distance of fibres in the experiment, the Rayleigh-Ritz method, and the numerical simulation.

6. Conclusion

The present paper focuses on studying the matrix shrinkage of the initial state of the virgin composite samples. The Rayleigh-Ritz method is employed to rapidly determine this matrix displacement field. The comparison of the maximum matrix shrinkage as a function of the distance of fibres with the experiment data is implemented for finding the fine parameters H , ν , ε^{In} .

Simulations on the 2D and 3D models of the problem are carried out on the Abaqus software for phenomenon validation. The numerical results of the matrix displacement were compared to the experiment and the Rayleigh-Ritz method. There is a good correlation between the results obtained by the two methods. Besides, 2D simulations can be used instead of 3D simulations because of an insignificant difference in the matrix displacements. Besides, the first damage will be predicted to occur in which the fibre-matrix interfaces intersect with the free edge.

Working in high and variable temperatures has been shown to cause mass loss, degradation of properties, shrinkage, and cracking on composite matrix. The main effect of a drop in temperature is causing the shrinkage phenomenon. Future research will consider the matrix shrinkage of aged samples in a thermal oxidation environment.

References

[1] X. Colin, C. Marais, J. Verdu, A new method for predicting the thermal oxidation of thermoset matrices: application to an amine crosslinked epoxy., *Polym Test*, vol. 20, no. 7, pp. 795-903, 2001.
[https://doi.org/10.1016/S0142-9418\(01\)00021-6](https://doi.org/10.1016/S0142-9418(01)00021-6)

[2] Anne Schieffer, Jean-Francois Maire, David L ev eque, A Coupled analysis of mechanical behaviour and ageing for polymer–matrix composites, *Compos Sci Technol*, vol. 62, no. 4, pp. 543-551, 2002.

[https://doi.org/10.1016/S0266-3538\(01\)00146-4](https://doi.org/10.1016/S0266-3538(01)00146-4)

- [3] M. C. Lafarie-Frenot, Damage mechanisms induced by cyclic ply-stresses in carbon–epoxy laminates: environmental effects, *Int Journal of Fatigue*, vol. 28, no. 10, pp. 1202-1218, 2006.
<https://doi.org/10.1016/j.ijfatigue.2006.02.014>
- [4] Kishore Pochiraju, Gyaneshwar Tandon, A. Schoeppner, Evolution of stress and deformations in high-temperature polymer matrix composites during thermo-oxidative aging, *Mech Time-Depend Mater*, vol. 12, no. 1, pp. 45-68, 2008.
<https://doi.org/10.1007/s11043-007-9042-5>
- [5] L. Olivier, N. Q. Ho, J. C. Grandier, M. C. Lafarie-Frenot, Characterization by ultra-micro indentation of an oxidized epoxy polymer: correlation with the predictions of a kinetic model of oxidation, *Polym Degrad Stab*, vol. 93, no. 2, pp. 489-497, 2008.
<https://doi.org/10.1016/j.polymdegradstab.2007.11.012>
- [6] S. Putthanarat, G. Tandon, G. A. Schoeppner, Influence of aging temperature, time, and environment on thermo-oxidative behavior of PMR-15: nanomechanical characterization., *J Mater Sci*, vol. 43, no. 20, pp. 714-723, 2008.
<https://doi.org/10.1007/s10853-008-2800-1>
- [7] G. A. Schoeppner, G. P. Tandon, E. R. Ripberger, Anisotropic oxidation and weight loss in PMR-15 composites, *Composites Part A*, vol. 38, no. 3, pp. 890-904, 2007.
<https://doi.org/10.1016/j.compositesa.2006.07.006>
- [8] S. Ciutacu, P. Budruga eac, I. Niculae, Accelerated thermal aging of glass-reinforced epoxy resin under oxygen pressure., *Polym Degrad Stab*, vol. 31, no. 3, pp. 365-372, 1991.
[https://doi.org/10.1016/0141-3910\(91\)90044-R](https://doi.org/10.1016/0141-3910(91)90044-R)
- [9] Tom Tsotsis, Scott Macklin Keller, K. Lee, Aging of polymeric composite specimens for 5000 hours at elevated pressure and temperature, *Compos Sci Technol*, vol. 61, no. 1, pp. 75-86, 2001.
[https://doi.org/10.1016/S0266-3538\(00\)00196-2](https://doi.org/10.1016/S0266-3538(00)00196-2)
- [10] Gigliotti M, Lafarie-Frenot M. C, Vu Dinh Quy, Experimental characterization of thermo-oxidation-induced shrinkage and damage in polymer-matrix composites, *Compos A Appl Sci Manuf.*, vol. 43, pp. 577-586, 2012.
<https://doi.org/10.1016/j.compositesa.2011.12.018>
- [11] Lafarie-Frenot M. C., Gigliotti M., Thermo-oxidation induced shrinkage in Organic Matrix Composites for High Temperature Applications: Effect of fiber arrangement and oxygen pressure, *Composite Structures*, vol. 146, pp. 176-86, 2016.
<https://doi.org/10.1016/j.compstruct.2016.03.007>
- [12] Gigliotti M., Minervino M., Lafarie-Frenot M. C., Assessment of thermo-oxidative induced chemical strain by inverse analysis of shrinkage profiles in unidirectional composites, *Composite Structures*, vol. 157, pp. 320-36, 2016.
<https://doi.org/10.1016/j.compstruct.2016.07.037>